The Canadian Mineralogist
Vol. 52, pp. 321-335 (2014)
DOI: 10.3749/canmin.52.2.321

ON THE GEOCHEMICAL CHARACTER OF PRIMARY Fe-Mn PHOSPHATES BELONGING TO THE TRIPHYLITE-LITHIOPHILITE, GRAFTONITE-BEUSITE, AND TRIPLITE-ZWIESELITE SERIES: FIRST RESULTS AND IMPLICATIONS FOR PEGMATITE PETROGENESIS

ENCARNACIÓN RODA-ROBLES AND ALFONSO PESQUERA

Departamento de Mineralogía y Petrología, Univ. País Vasco (UPV/EHU), P.O. Box 644, E–48080, Bilbao, Spain

SONIA GARCÍA DE MADINABEITIA

SGIker-Geochronology, UPV/EHU, Spain

JOSÉ-IGNACIO GIL IBARGUCHI

Departamento de Mineralogía y Petrología, Univ. País Vasco (UPV/EHU), P.O. Box 644, E–48080, Bilbao, Spain

JIM NIZAMOFF, WILLIAM SIMMONS, AND ALEXANDER FALSTER

Department of Earth and Environmental Sciences, University of New Orleans, 2000 Lakeshore Drive, New Orleans, Louisiana 70148, US

MIGUEL ANGEL GALLISKI

IANIGLA, CCT–MENDOZA CONICET, Avda. Ruiz Leal s/n, Parque Gral. San Martín, C.C. 330, (5.500) Mendoza, Argentina

ABSTRACT

Iron-Mn phosphate minerals are common accessory phases in pegmatites, some granites and, rarely, in some hydrothermal quartz-rich dikes. A comprehensive textural and geochemical characterization of primary phosphate minerals belonging to the triplite-zwieselite, triphylite-lithiophilite, and graftonite-beusite series has been done. Chemical data, including major and trace elements contents, have been obtained by electron microprobe (EMP) and laser-ablation inductively coupled-plasma mass-spectrometry (LA-ICP-MS) techniques. The concentration of trace elements shows important differences for the three series of primary Fe-Mn phosphate minerals. Members of the triphylite-lithiophilite series are the poorest in trace elements, with Zn as the only element that may occur in important amounts. This low concentration in trace elements could be related to structural constrains. Graftonite-beusite members are the richest in REE, most probably due to the substitution of Ca by the rare earths. Members of the triplite-zwieselite series are the richest in certain HFSE, such as Nb and Ta. There is an important difference in the shape of multi-element diagrams of triplite-zwieselite samples associated with pegmatites, all of them showing a strong negative Eu anomaly, and those of samples from a quartz-rich dike, with no Eu anomaly. This difference is interpreted as the result of the Eu fractionation in pegmatites due to the previous crystallization of plagioclase.

No correlation has been found between the Fe/(Fe+Mn) ratio and the different trace element contents of the primary phosphate series. Moreover, the concentrations of trace elements are not simply related to the pegmatite type, its paragenesis or its geological setting. Further investigation of mineral association, textural relationships, partition coefficients, and geology and history of crystallization of the pegmatitic bodies appears necessary in order to determine the factors controlling the variability in the trace elements content for the different primary phosphate series.

Keywords: phosphates, trace elements, pegmatites, laser-ablation inductively coupled-plasma mass-spectrometry.

§ *Corresponding author e-mail address*: encar.roda@ehu.es

Introduction

Iron-Mn phosphates are common accessory mineral phases in pegmatites and some granites, particularly in the beryl-columbite-phosphate pegmatite subtype of Černý & Ercit (2005). They also occur in some hydrothermal quartz-rich dikes (*e.g.*, Garate-Olabe *et al.* 2012). Like for other minerals (*e.g.*, micas, K-feldspars), the chemical composition of phosphate minerals has been used to establish the degree of evolution of the pegmatites in which they occur: a decrease of the Fe/(Fe+Mn) ratio in primary phosphate minerals has been associated with an increasing differentiation degree of pegmatites (Ginsburg 1960, Fransolet *et al.* 1986, Keller *et al.* 1994, Roda *et al.* 2005, Roda-Robles *et al.* 2010). This ratio, however, depends on the presence of other Fe-(Mg-Mn)-rich minerals, such as tourmaline, biotite, and/or garnet, and, consequently, it must be used with caution as indicator of differentiation degree of pegmatites (London & Burt 1982, London 2008, Roda-Robles *et al.* 2012). Trace element geochemistry has contributed significantly to deciphering the physical and chemical processes (*e.g.*, partial melting, fractionation, role of fluids, contamination) in the evolution of magmatic rocks. Hence, a more complete chemical characterization including trace elements could help lead to a better understanding of the role that phosphate minerals play in the evolution of pegmatites.

This work presents preliminary results regarding trace element content and geochemical features of primary Fe-Mn phosphate minerals occurring in pegmatitic rocks. These results will help us decipher the behavior of primary phosphate minerals and the distribution of trace elements among melt, major and minor phases in these rocks. To this purpose, phosphate minerals belonging to the triplite-zwieselite, triphylite-lithiophilite, and graftonite-beusite series were analyzed by electron microprobe (EMP) and laser-ablation inductively coupled-plasma mass-spectrometry (LA-ICP-MS) techniques. We have examined the chemical variation of these primary phosphate minerals and their different textural relationships in several pegmatites. We have also evaluated the crystal-chemical and geochemical factors which may control the trace elements content in phosphates.

Selected Materials

The selected primary phosphate minerals belong to the triplite-zwieselite $(Mn^{2+},Fe^{2+},Mg,Ca)_2(PO_4)(F,OH)$, triphylite-lithiophilite $Li(Fe^{2+},Mn^{2+})PO_4$, and graftonite-beusite $(Fe^{2+},Mn^{2+},Ca)_3(PO_4)_2$ series. The samples originate from one quartz dike in Portugal and from 14 different pegmatites from Argentina, Germany, Portugal, Spain, and the USA (Table 1). Nine of these pegmatites belong to the beryl type (beryl-columbite-phosphate subtype) of Černý & Ercit (2005), whereas five of them belong to the complex type of the same classification (Table 1). Eight samples of the triplite-zwieselite series, six of the triphylite-lithiophilite series, and five of the beusite-graftonite series were analyzed.

Members of the triplite-zwieselite series are common phosphate mineral phases in pegmatites and also in some quartz dikes (Table 1). In hand sample, the studied specimens appear as dense masses up to 70 cm in diameter, with a dark brownish color, locally reddish. Luster is vitreous and crystals are more transparent in these reddish areas. Fracture is conchoidal to irregular. Under the microscope, when fresh, triplite-zwieselite crystals appear as quite homogeneous colorless to yellowish, anhedral grains, with grayish interference color and a granular to massive texture (Fig. 1a). In some of the samples, inclusions are locally abundant (Fig. 1a). In those cases, in order to avoid contamination of the chemical analyses, data were always collected from the cleanest areas, where no inclusions were observed. Spherulitic phosphosiderite is the most common alteration product of the triplite-zwieselite members (Fig. 1b).

Masses up to 1 m in diameter of triphylite-lithiophilite members occur as the main primary phosphate mineral in many pegmatites, both beryl and complex types (Table 1). Color in hand sample ranges from grayish to beige, whereas some light greenish-yellowish samples are rare. Luster is subvitreous and fracture is irregular. Under the microscope, members of the triphylite-lithiophilite series may present different textures. The simplest are similar to the ones described above for triplite-zwieselite, are granular or massive in texture, and are composed of homogenous, colorless, and anhedral crystals of triphylite-lithiophilite (Fig. 1c). However, typically, triphylite-lithiophilite crystals present numerous lenticular or irregular lamellae of sarcopside that show two preferential crystallographic orientations (Fig. 1d). Intergrowths of graftonite containing coarse lamellae of triphylite-lithiophilite are less abundant (Fig. 1e). Most lamellae are platy and form a single set that share a quite uniform optical orientation, enclosed in monocrystalline graftonite, giving rise to a laminated parallel intergrowth (Fig. 1e) that is interpreted by the authors to be the result of the simultaneous crystallization of the two phases. Members of the triphylite-lithiophilite series are easily altered, mainly on the surface, by Li-leaching and a simultaneous progressive oxidation of the transition cations Fe^{2+} and Mn^{2+}. The products of this alteration are ferrisicklerite-sicklerite and heterosite-purpurite in succession, following the oxidation sequence first described by Quensel (1937) and Mason (1941) (Fig. 1c). Other common replacement products include members of the alluaudite-varulite and staněkite-joosteite series.

Members of the graftonite-beusite series are mainly common in the beryl-columbite-phosphate pegmatites

TABLE 1. MAIN CHARACTERISTICS OF THE PRIMARY PHOSPHATE MINERALS STUDIED AND THEIR HOSTING PEGMATITES

Locality/rock type	Country rock	Main minerals	Phosphate association	Phosphate textures	Fe/(Fe+Mn) Trpl-Grf-Trph		
Folgosinho (Guarda, Portugal) **Quartz-hydrothermal dyke**	granodiorite	Qtz, Ms, Phosph, Aspy, Py, Tur, Grt	Trpl, Phs, Ap, Hur	massive masses of Trpl, up to 30 cm of diameter	0.47	-	-
Gigante (Córdoba, Argentina) **Beryl type pegmatite**	porphyritic granite	Qtz, Mic, Ab, Ms, Brl, CGM, Zrn, Sps, Ura	Trpl, F-Ap, Cyr, Eos, Flue, Gall, Gay	Trpl massive nodules with color zoning including F-Ap	0.32	-	-
El Criollo (Córdoba, Argentina) **Beryl type pegmatite**	porphyritic granite	Qtz, Mic, Ab, Mu, Brl, CGM, Bt, Py, Cpy	Trpl, F-Ap, Eos, Flue	Trpl massive nodules with color zoning, including F-Ap	0.41	-	-
Hagendorf Süd (Bavaria, Germany) **Beryl type pegmatite**	metapelites	Qtz, Pl, Kfs, Ms, Bt, Brl, Phs, CGM	Trph, Src, Zws, Fsk, Grf, Wolf	Src lamellae inside granoblastic Trph Zws massive nodules	0.54	-	n.d.
Black Beauty (Colorado, USA) **Beryl type pegmatite**	mica schist granitic gniess	Qtz, Kfs, Ms, Bt, Brl, Phosph	Trpl, Ap	massive nodules of Trpl	0.32	-	-
Mica Lode (Colorado, USA) **Beryl type pegmatite**	quartz-mica schist	Qtz, Pl, Kfs, Ms, Bt, Brl, Grt, Phosph, CGM	Trpl, Ap	brown masses and rough crystals up to 20 cm length of Trpl	0.22	-	-
Tourmaline Queen (California, USA) **Complex type pegmatite**	gabbro	Qtz, Pl, Kfs, Ms, Bt, Lpd, Brl, Grt, Srl, Elb, Spd, Phosph, CGM	Lph, Trpl, F-Ap	granoblastic Lph, massive Trpl	0.12	-	n.d.
Swanson (Connecticut, USA) **Complex type pegmatite**	metasediments	Qtz, Kfs. Pl, Ms, Lpd, Grt, Brl, Bt, Cst, CGM, Phosph, Srl	Trpl	Trpl intergrowth with Tur	0.04	-	-
Storm Mountain (Colorado, USA) **Beryl type pegmatite**	mica schist	Qtz, Ms, Kfs, Pl, Brl, Srl, Grt, Phosph	Beu, Ap	massive nodules of Beu	-	0.42	1
Keystone (South Dakota, USA) **Complex type pegmatite**	quartz-mica schist	Qtz, Ms, Kfs, Pl, Brl, Spd, CGM, Cst, Phosph	Beu, Trph, Arroj, Wyl	massive nodules of Trph and Beu	-	0.49–n.d.	
Cema (San Luis, Argentina) **Complex type pegmatite**	schists	Qtz, Pl, Kfs, Ms, Tur, Grt, Brl, Phosph, Spd	Sk, Beu, Vr, Qng, Ap, Joo	granoblasitc Sk and Beu	-	0.36–0.38	
Palermo-1 (New Hampshire, USA) **Beryl type pegmatite**	schists	Qtz, Pl, Kfs, Ms, Brl, Phosph ± Tur	Grf, Trph, Fsk	Trph/fsck lamellae inside Grf. Granoblastic Grf and Trph/Fsk	-	0.64–0.81	
Cañada (Salamanca, Spain) **Beryl type pegmatite**	leucogranite & gabbro	Qtz, Pl, Kfs, Ms, Brl, Tur, Phosph, Grt	Trph, Src, Fsk, Grf, Wolf, Mtb	Src lamellae inside granoblastic Trph Granoblastic Grf	-	0.61–0.80	
NªSª de Assunçao (Aguiar da Veira, Portugal) **Beryl type pegmatite**	two-mica granite	Qtz, Pl, Kfs, Ms, Bt, Brl, Phosph	Trph, Src, Trpl, Iso, Ap	Src lamellae inside granoblastic Trph	n.d.	-	0.52
Emmons (Maine, USA) **Complex type pegmatite**	migmatites	Qtz, Pl, Kfs, Ms, Tur, Brl, Pollc, Spd, CGM	Lph, Sk, Ap, Mtb	euhedral crystals up to 8 cm in length	-	-	0.36

Symbols used: Ab: albite, Ap: apatite, Arroj: arrojadite, Aspy: arsenopyrite, Beu: Beusite, Brl: beryl, Bt: biotite, CGM: columbite-group minerals, Cpy: chalcopyrite, Cst: cassiterite, Cyr: cyrilovite, Elb: elbaite, Eos: eosphorite, F-Ap: F-apatite, Flue: fluellite, Fsk: ferrisicklerite, Gall: galliskite, Gay: gayite, Grf: graftonite, Grt: garnet, Hur: hureaulite, Iso: isokite, Joo: joosteite, Kfs: K feldspar, Lpd: lepidolite, Lph: lithiophilite, Mic: microcline, Ms: muscovite, Mtb: montebrasite, Phosph: phosphates, Phs: phosphosiderite, Pl: plagioclase, Pollc: pollucite, Py: pyrite, Qng: qingheiite, Qtz: quartz, Sk: sicklerite, Spd: spodumene, Sps: spessartine, Src: sarcopside, Srl: schorl, Trph: triphylite, Trpl: triplite, Tur: tourmaline, Ura: uraninite, Vr: varulite, Wolf: wolfeite, Wyl: wyllieite, Zrn: zircon, Zws: zwieselite. n.d.: not determined. In the rock type, pegmatite classification according to Černý & Ercit (2005).

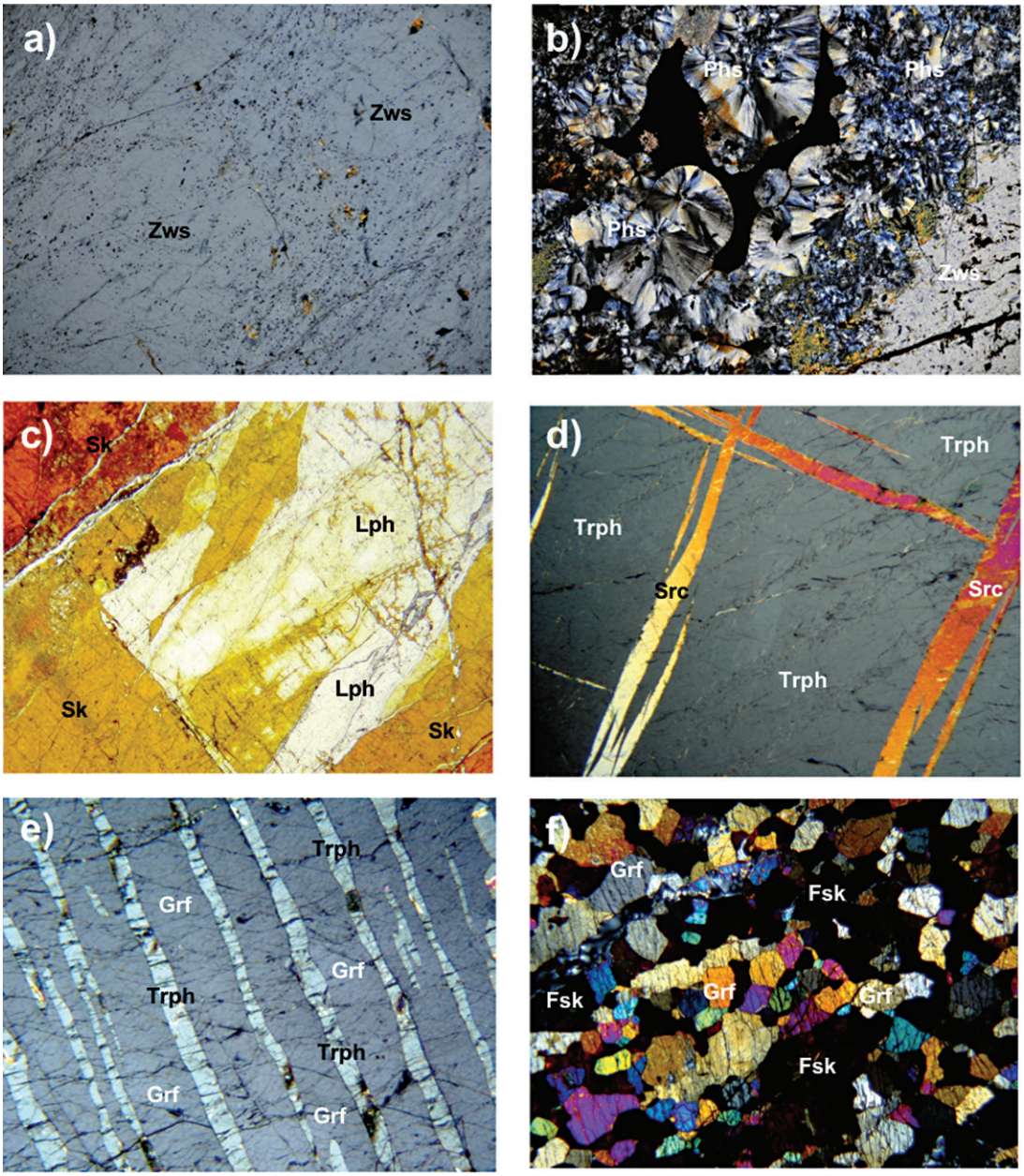

FIG. 1. Photomicrographs of the main textures presented by the primary phosphate minerals studied in this work: (a) fresh triplite crystals from the El Criollo pegmatite, with a massive texture, showing locally numerous inclusions, crossed polars; (b) zwieselite crystals partly replaced by spherulitic grains of phosphosiderite from the Folgosinho quartz dike, crossed polars; (c) massive crystals of lithiophilite (colorless), partially replaced by sicklerite (orange) from the Cema pegmatite, plane polarized light; (d) lenticular lamellae of sarcopside in massive triphylite—these lamellae show two preferential crystallographic orientations corresponding to the cleavage planes of triphylite—from the Cañada pegmatite, crossed polars; (e) intergrowths of coarse platy lamellae of triphylite in massive graftonite from the Palermo 1 pegmatite, crossed polars; and, (f) graftonite and ferrisicklerite granular subhedral crystals in a granoblastic texture from the Palermo 1 pegmatite. Size of the pictures is 1.7 × 2.6 mm. Symbols: Fsk – ferrisicklerite, Grf – graftonite, Lph – lithiophilite, Phs – phosphosiderite, Sk – sicklerite, Src – sarcopside, Trph – triphylite, Zws – zwieselite.

subtype of the beryl type, whereas in the complex type they are less common. Two samples from every pegmatite type were included in this study (Table 1). In hand sample, the graftonite-beusite members rarely occur in monomineralic masses. They mostly occur associated with other phosphate minerals, usually those of the triphylite-lithiophilite series. Color is dark, from brownish to near black, with an earthy to subvitreous luster and irregular fracture. Under the microscope, besides the platy intergrowths previously described (Fig. 1e), graftonite typically appears as granular subhedral crystals in a granoblastic texture (Fig. 1f).

Analytical Techniques

Characterization of the phosphate minerals was carried out *via* study of their optical properties in thin section, X-ray powder-diffraction, electron-microprobe, and LA-ICP-MS techniques. More than 650 microprobe compositions (325 from triplite-zwieselite grains, 144 from graftonite-beusite, and 190 from triphylite-lithiophilite) were obtained at the Université Paul Sabatier (Toulouse, France), with a Cameca SX 50 electron microprobe. The operating conditions were: voltage of 15 kV and beam current of 10 nA for all elements. The following natural and synthetic minerals were used as standards: graftonite (P), corundum (Al), hematite (Fe), pyrophanite (Mn and Ti), periclase (Mg), wollastonite (Ca), sanidine (K), albite (Na), fluorite (F), and tugtupite (Cl). Analyses of trace elements in phosphate minerals were conducted by laser-ablation inductively coupled-plasma mass-spectrometry (LA-ICP-MS) at the Geochronology and Isotope Geochemistry-SGIker facility of the University of the Basque Country (Spain). The analyses involved the ablation of minerals in *ca*. 60 μm thick petrographic sections with an UP213 Nd:YAG laser ablation system (New Wave) coupled to a Thermo Fisher Scientific XSeries 2 quadrupole ICP-MS instrument with sensitivity enhanced through a dual pumping system. Spot diameters of *ca*. 100 μm associated with repetition rates of 10 Hz and laser fluence at the target of *ca*. 5.5 J/cm^2 were used for analysis. The ablated material was carried in He and then mixed with Ar. Tuning and mass calibration were performed using the NIST SRM 612 reference glass, by inspecting the signal of ^{238}U to obtain *ca*. 14,000,000 cps/ppm, and by minimizing the ThO^+/Th^+ ratio to *ca*. 1%. Raw data were processed using Iolite 2.3 (Paton *et al*. 2011, Paul *et al*. 2012) and Ca as internal standard (determined by electron microprobe). The procedure was optimized using apatite from Cerro Mercado (Durango, Mexico). The same mineral was used as a secondary standard to control the quality of the results in each analytical session. Once the method was established, around 400 LA-ICP-MS analyses were done on eight samples of the triplite-zwieselite series, six of the triphylite-lithiophilite, and five of the graftonite-beusite series from 14 pegmatites and 1 hydrothermal quartz dike, covering the widest possible Fe-Mn compositional range for each series.

Results

Major and trace element contents and the calculated empirical formulae of samples belonging to the three series of primary phosphate minerals are given in Tables 2, 3, and 4. Regarding the major elements, the Fe/(Fe+Mn) ratios are in the ranges 0.04–0.56, 0.36–0.81, and 0.35–065 for the analyzed triplite-zwieselite, triphylite-lithiophilite, and graftonite-beusite series, respectively. Members of the graftonite-beusite series also show important differences in the Ca content, with the highest values found in some graftonite crystals from the Palermo pegmatite (13.74 wt.% CaO, 0.848 Ca *apfu*) and the lowest values belonging to the beusite from the Keystone pegmatite (5.58 wt.% CaO, 0.361 Ca *apfu*). In the triplite-zwieselite series, the F content varies over a smaller range, between 3.35 wt.%, for the zwieselite from Hagendorf-Süd, and 5.55 wt.%, for the triplite from the Swanson pegmatite.

The trace element contents show important variations among members of the studied series of primary Fe-Mn phosphate minerals (Tables 2, 3, 4; Figs. 2, 3, 4). However, samples belonging to the same series show fairly similar shapes in trace element diagrams normalized to the concentrations of total continental crust (Rudnick & Fountain 1995), whereas significant differences are observed among the three phosphate mineral series (Fig. 2). In order to evaluate possible correlations among the different pairs of elements in the three series, a correlation matrix was made, which also included the Fe/(Fe+Mn) values.

In detail, the members of the triphylite-lithiophilite series contain extremely low amounts of all the analyzed trace elements, except for Zn, which shows values in the range of 570–800 ppm for the samples from the Cema, Palermo, and Cañada pegmatites, 1630–1860 ppm for those samples from the Emmons pegmatite, and the highest values of 1400–8990 ppm for phosphate crystals found in the Nossa Senhora de la Assunçao pegmatite (Table 2, Fig. 2a). The samples analyzed show a wide range of Li content, which could be related to different degrees of leaching of Li from the primary triphylite, giving intermediate values between triphylite and ferrisicklerite. All the compositions given in Table 2 belong to crystals that were colorless under the microscope, which was taken by the authors as a criterion to discriminate between triphylite-lithiophilite and ferrisicklerite-sicklerite. However, in all the cases it was necessary to include some Fe^{3+} to maintain charge balance. No correlation has been found between the Fe/(Fe+Mn) ratio and any trace element in this series.

Samples of the triplite-zwieselite series are, overall, richer in trace elements than those of the triphylite-

TABLE 2. CHEMICAL COMPOSITION OF THE MEMBERS OF THE TRIPHYLITE-LITHIOPHILITE SERIES FROM DIFFERENT PEGMATITES

Sample		PAL-74	PAL-84	CAÑ-27	CAÑ-54	CAÑ-64	NSAS-15	NSAS-24	NSAS-34	CEM-35	CEM-56	CEM-65	CEM-75	EMM-35	EMM-46	EMM-56
P_2O_5	wt.%	45.30	43.31	45.37	44.31	44.72	45.49	45.37	44.41	45.33	45.40	45.75	45.45	45.27	45.56	45.14
Al_2O_3		<0.01	<0.01	0.01	<0.01	<0.01	0.01	<0.01	<0.01	0.01	0.01	<0.01	0.01	0.01	<0.01	0.01
TiO_2		<0.01	<0.01	<0.01	<0.01	<0.01	<0.01	<0.01	<0.01	<0.01	<0.01	<0.01	<0.01	<0.01	<0.01	<0.01
MgO		1.70	1.68	1.20	1.17	1.29	0.03	0.01	0.01	0.43	0.48	0.50	0.50	0.13	0.14	0.18
FeO(tot)		35.23	35.11	35.31	35.52	35.09	23.98	23.52	23.34	16.83	16.94	16.67	16.83	16.58	16.20	16.32
MnO		8.54	8.38	8.89	8.51	8.69	21.62	21.65	21.99	27.32	27.50	27.65	27.57	28.39	28.42	28.73
CaO		0.01	0.02	0.02	0.02	0.02	0.01	0.01	<0.01	0.01	<0.01	0.01	<0.01	0.02	0.04	0.05
Na_2O		<0.01	0.04	0.04	0.04	0.02	0.02	0.01	0.02	0.01	0.02	0.03	0.01	0.04	<0.01	0.02
K_2O		<0.01	0.01	0.01	<0.01	0.01	0.01	<0.01	<0.01	<0.01	<0.01	0.02	<0.01	<0.01	<0.01	<0.01
Li_2O		6.04	6.05	6.20	5.98	6.37	3.12	3.66	5.16	7.48	7.09	6.86	6.73	8.07	4.96	4.68
TOTAL		90.78	88.55	90.86	89.58	89.84	91.18	90.59	89.77	89.96	90.38	90.64	90.4	90.44	90.39	90.46
P	*apfu*	1	1	1	1	1	1	1	1	1	1	1	1	1	1	1
Al		<0.001	<0.001	<0.001	<0.001	<0.001	<0.001	<0.001	<0.001	<0.001	<0.001	<0.001	<0.001	<0.001	<0.001	<0.001
Ti		<0.001	<0.001	<0.001	<0.001	<0.001	<0.001	<0.001	<0.001	<0.001	<0.001	<0.001	<0.001	<0.001	<0.001	<0.001
Mg		0.066	0.069	0.047	0.047	0.051	<0.001	<0.001	<0.001	0.017	0.019	0.020	0.020	0.005	0.005	0.007
Fe^{++++*}		0.320	0.207	0.324	0.294	0.280	0.677	0.636	0.417	0.241	0.270	0.318	0.311	0.161	0.519	0.501
Fe^{++}		0.768	0.801	0.769	0.793	0.775	0.521	0.512	0.520	0.367	0.369	0.360	0.366	0.362	0.351	0.357
Mn^{++}		0.189	0.194	0.196	0.192	0.195	0.476	0.478	0.496	0.603	0.606	0.605	0.607	0.628	0.624	0.637
Ca		<0.001	<0.001	<0.001	0.001	0.001	<0.001	<0.001	<0.001	0.001	<0.001	<0.001	<0.001	<0.001	0.001	0.001
Na		<0.001	0.002	0.002	0.002	0.001	0.001	0.001	0.001	<0.001	0.001	0.002	0.001	0.002	<0.001	0.001
K		<0.001	<0.001	<0.001	<0.001	<0.001	<0.001	<0.001	<0.001	<0.001	<0.001	0.001	<0.001	<0.001	<0.001	<0.001
Li		2.639	2.726	2.706	2.664	2.805	1.422	1.665	2.329	3.234	3.070	2.968	2.927	3.457	2.211	2.103
Fe/(Fe+Mn)		0.80	0.81	0.80	0.80	0.80	0.52	0.52	0.52	0.38	0.38	0.38	0.38	0.37	0.36	0.36
Fe/(Fe+Mg)		0.92	0.92	0.94	0.95	0.94	1.00	1.00	1.00	0.95	0.95	0.95	0.95	0.98	0.99	0.98
n		3	3	3	3	3	3	3	3	3	3	3	3	3	3	3
Sc	ppm	0.76	0.84	46.48	49.19	54.00	1090.67	969.33	1001.67	Bdl	Bdl	0.12	Bdl	0.28	0.25	0.26
V		Bdl	0.01	Bdl	Bdl	Bdl	2.89	Bdl	0.15	Bdl	0.01	Bdl	0.27	Bdl	Bdl	<0.01
Cr		0.17	0.16	0.21	0.19	0.22	1.18	0.72	1.34	0.19	0.19	0.21	0.22	0.24	0.22	0.22
Co		0.60	0.59	1.53	1.75	1.92	2.70	2.30	3.45	0.20	0.46	0.25	0.42	0.13	0.19	0.19
Ni		0.02	Bdl	0.02	0.04	0.03	0.79	0.06	0.21	Bdl	Bdl	Bdl	0.02	Bdl	Bdl	Bdl
Cu		<0.01	<0.01	<0.01	<0.01	<0.01	<0.01	<0.01	<0.01	Bdl	<0.01	Bdl	Bdl	Bdl	Bdl	<0.01
Zn		648	635	693	621	662	3747	4593	6763	596	594	600	768	1748	1683	1635
Rb		Bdl	Bdl	Bdl	0.01	Bdl	0.99	Bdl	0.21	0.17	0.03	0.01	0.06	0.23	0.02	0.16
Sr		0.02	0.02	0.01	0.02	0.02	1.85	0.40	0.68	0.10	0.06	0.04	3.01	0.05	0.05	0.04
Y		0.01	0.02	<0.01	<0.01	0.01	2.22	1.95	2.28	0.01	0.01	0.01	0.05	0.01	0.01	0.02
Zr		0.01	0.01	<0.01	Bdl	0.01	1.69	0.47	0.27	<0.01	<0.01	Bdl	0.01	<0.01	<0.01	0.01
Nb		0.01	<0.01	0.02	0.07	0.06	1.14	0.01	0.02	0.01	Bdl	<0.01	0.01	0.01	<0.01	0.02
Ba		Bdl	Bdl	Bdl	Bdl	0.02	1.51	0.62	0.66	0.35	Bdl	Bdl	0.20	Bdl	Bdl	Bdl
La		0.01	0.09	<0.01	Bdl	0.01	1.11	0.04	0.18	<0.01	Bdl	<0.01	0.18	<0.01	0.01	0.01
Ce		0.01	0.07	<0.01	Bdl	0.01	1.06	0.05	0.19	<0.01	<0.01	<0.01	0.18	<0.01	0.01	0.01
Pr		0.01	0.01	Bdl	Bdl	0.01	1.13	0.03	0.13	<0.01	<0.01	<0.01	0.02	<0.01	<0.01	<0.01
Nd		0.01	Bdl	Bdl	Bdl	0.01	1.03	0.04	0.18		Bdl	<0.01	0.06	Bdl	0.01	<0.01
Sm		<0.01	<0.01	Bdl	Bdl	<0.01	1.14	0.01	0.06		Bdl	<0.01	0.01	Bdl	<0.01	<0.01
Eu		<0.01	<0.01	<0.01	<0.01	<0.01	0.91	0.01	0.02	<0.01	<0.01	<0.01	0.01	<0.01	<0.01	<0.01
Gd		<0.01	<0.01	<0.01	<0.01	<0.01	1.41	0.03	0.08	<0.01	<0.01	<0.01	0.01	<0.01	<0.01	<0.01
Tb		<0.01	<0.01	<0.01	<0.01	<0.01	0.98	0.02	0.02	<0.01	Bdl	<0.01	0.01	<0.01	<0.01	<0.01
Dy		<0.01	<0.01	<0.01	<0.01	<0.01	1.19	0.21	0.30	<0.01	<0.01	<0.01	0.01	<0.01	Bdl	<0.01
Ho		<0.01	<0.01	<0.01	<0.01	<0.01	1.18	0.04	0.07	<0.01	<0.01	<0.01	0.01	<0.01	<0.01	<0.01
Er		<0.01	<0.01	<0.01	<0.01	<0.01	1.36	0.10	0.16	<0.01	<0.01	<0.01	0.01	<0.01	<0.01	<0.01
Tm		<0.01	<0.01	<0.01	<0.01	<0.01	1.21	0.02	0.04	Bdl	Bdl	<0.01	0.01	<0.01	<0.01	<0.01
Yb		0.01	<0.01	0.07	0.09	0.10	1.14	0.18	0.32	<0.01	Bdl	<0.01	0.01	<0.01	Bdl	<0.01
Lu		<0.01	<0.01	0.02	0.02	0.02	1.17	0.03	0.05	<0.01	<0.01	<0.01	0.01	<0.01	<0.01	<0.01
Hf		<0.01	<0.01	<0.01	Bdl	<0.01	0.97	0.01	0.02	Bdl	Bdl	Bdl	<0.01	<0.01	Bdl	<0.01
Ta		<0.01	<0.01	0.01	0.08	0.04	1.06	0.01	0.02	0.03	0.01	<0.01	0.01	0.02	Bdl	<0.01

Sample	PAL-7	PAL-8	CAÑ-2	CAÑ-5	CAÑ-6	NSAS-1	NSAS-2	NSAS-3	CEM-3	CEM-5	CEM-6	CEM-7	EMM-3	EMM-4	EMM-5
n	4	4	7	4	4	5	4	4	5	6	5	5	5	6	6
Pb	Bdl	Bdl	0.01	Bdl	Bdl	0.80	0.13	0.12	0.28	0.01	Bdl	0.14	Bdl	Bdl	Bdl
Th	<0.01	0.01	<0.01	<0.01	0.01	1.11	0.02	0.12	<0.01	<0.01	<0.01	0.02	<0.01	<0.01	<0.01
U	<0.01	<0.01	<0.01	<0.01	<0.01	0.85	<0.01	0.02	<0.01	<0.01	<0.01	0.01	<0.01	<0.01	<0.01
ΣLREE	0.02	0.02	<0.01	<0.01	0.04	5.47	0.17	0.73	<0.01	<0.01	<0.01	0.45	<0.01	0.03	0.02
ΣHREE	0.02	0.02	0.09	0.12	0.14	10.55	0.65	1.05	<0.01	<0.01	<0.010	0.08	0.01	<0.01	0.01

Data of major elements obtained by electron microprobe, except for Li_2O, calculated by LA-ICP-MS. Data of trace elements obtained by ICP-MS-LA techniques. The data reported are an average result on n point analyses. The cation numbers are calculated on the basis of 1P per formula unit. Localities: PAL: Palermo 1 pegmatite, CAÑ: Cañada pegmatite, NSA: Nª Sª de la Assunçao, CEM: Cema, EMM: Emmons. Bdl: below detection limits. * Fe^{+++} apfu values calculated to maintain the charge balance. All the samples analyzed correspond to colorless areas of the crystals under the microscope.

TABLE 3. CHEMICAL COMPOSITION OF MEMBERS OF THE TRIPLITE-ZWIESELITE SERIES FROM DIFFERENT PEGMATITES

Sample		SWA-3	SWA-8	SWA-14	T-Q-1	T-Q-2	T-Q-4	M-L-2	M-L-5	M-L-1	B-B-3	B-B-4	B-B-5
n		10	10	10	10	11	10	11	10	12	10	11	10
P_2O_5	wt.%	30.94	30.79	30.59	30.61	30.62	30.46	33.80	33.73	31.94	31.29	33.89	31.75
Al_2O_3		0.01	0.01	0.01	0.01	0.01	0.02	0.02	0.05	0.01	<0.01	0.01	0.01
MgO		0.01	<0.01	0.02	0.04	0.03	0.03	9.69	9.60	4.35	4.43	3.59	4.62
FeO		2.44	2.23	2.41	7.47	8.00	7.12	11.41	11.67	18.02	18.23	14.64	18.09
MnO		57.88	58.16	58.19	55.57	54.92	55.51	39.73	39.61	38.19	38.07	30.64	38.10
CaO		2.69	2.83	2.75	0.38	0.36	0.36	1.20	1.20	0.92	1.04	11.69	0.89
Na_2O		0.02	0.02	0.02	0.02	0.03	0.01	0.01	<0.01	0.01	0.02	0.01	0.02
K_2O		<0.01	<0.01	<0.01	<0.01	<0.01	<0.01	<0.01	<0.01	<0.01	<0.01	<0.01	<0.01
F		4.89	4.80	4.90	4.54	4.36	4.48	4.65	4.45	4.32	4.37	4.10	4.33
Cl		<0.01	<0.01	<0.01	<0.01	<0.01	<0.01	<0.01	<0.01	<0.01	<0.01	<0.01	<0.01
TOTAL		98.90	98.85	98.88	98.65	98.31	97.99	100.51	100.31	97.77	97.46	98.58	97.81
O = F		2.06	2.02	2.06	1.91	1.84	1.89	1.96	1.87	1.82	1.84	1.73	1.83
total		96.84	96.83	96.81	96.74	96.47	96.10	98.55	98.43	95.95	95.62	96.85	95.99
P	*apfu*	1.000	1.000	1.000	1.000	1.000	1.000	1.000	1.000	1.000	1.000	1.000	1.000
Al		0.001	<0.001	<0.001	<0.001	<0.001	0.001	0.001	0.002	<0.001	<0.001	<0.001	<0.001
Mg		0.001	<0.001	0.001	0.002	0.002	0.002	0.505	0.501	0.240	0.249	0.187	0.256
Fe++		0.078	0.072	0.078	0.241	0.258	0.231	0.333	0.342	0.557	0.576	0.427	0.563
Mn		1.871	1.890	1.903	1.816	1.794	1.823	1.176	1.175	1.196	1.217	0.905	1.200
Ca		0.110	0.117	0.114	0.016	0.015	0.015	0.045	0.045	0.037	0.042	0.437	0.035
Na		0.001	0.002	0.002	0.001	0.002	0.001	0.001	<0.001	0.001	0.001	0.001	0.001
K		<0.001	<0.001	<0.001	<0.001	<0.001	<0.001	<0.001	<0.001	<0.001	<0.001	<0.001	<0.001
F		0.591	0.583	0.599	0.554	0.532	0.550	0.513	0.493	0.505	0.522	0.452	0.512
Cl		<0.001	<0.001	<0.001	<0.001	<0.001	<0.001	<0.001	<0.001	<0.001	<0.001	<0.001	<0.001
Fe/(Fe+Mn)		0.04	0.04	0.04	0.12	0.13	0.11	0.22	0.23	0.32	0.32	0.32	0.32
Fe/(Fe+Mg)		0.99	1.00	0.99	0.99	0.99	0.99	0.40	0.41	0.70	0.70	0.70	0.69
n		5	5	5	5	5	5	5	5	5	5	5	5
Li	ppm	5.68	16.24	8.41	14.32	19.15	21.33	20.42	19.14	3.81	2.02	2.33	4.67
Sc		0.44	0.54	0.50	0.55	0.52	0.57	1.16	1.16	4.77	4.24	4.06	5.34
V		<0.01	<0.01	<0.01	0.06	<0.01	<0.01	0.04	0.04	0.18	0.24	0.23	0.22
Cr		0.36	0.39	0.47	0.58	0.75	0.90	0.35	0.36	0.87	0.77	0.74	0.86
Co		<0.01	<0.01	<0.01	<0.01	<0.01	<0.01	5.01	4.85	7.14	6.88	6.39	8.52
Ni		<0.01	<0.01	<0.01	<0.01	<0.01	<0.01	0.07	0.11	2.59	2.63	2.29	2.89
Cu		<0.01	<0.01	<0.01	<0.01	<0.01	<0.01	<0.01	<0.01	0.22	0.17	0.21	0.16
Zn		437	541	610	1771	1937	2526	4047	3945	1301	1539	1625	1848
Rb		0.16	<0.01	0.08	0.17	0.20	0.09	<0.01	0.01	0.06	0.04	0.12	0.21
Sr		7.88	0.08	0.11	4.04	1.14	0.02	0.59	3.43	2.32	6.81	6.85	0.98
Y		0.73	0.85	0.92	1.44	0.54	0.45	53.17	54.47	32.90	43.80	51.70	21.2
Zr		16.37	6.43	18.23	42.06	47.20	54.52	124.53	123.63	44.66	68	65.66	19.42

Sample		SWA-3	SWA-8	SWA-14	T-Q-1	T-Q-2	T-Q-4	M-L-2	M-L-5	M-L-1	B-B-3	B-B-4	B-B-5
n		10	10	10	10	11	10	11	10	12	10	11	10
Nb		88.14	89.86	107.20	276.80	339.00	378.60	512.23	498.71	164.20	140.65	150.56	99.80
Ba		4.16	<0.01	0.19	<0.01	<0.01	<0.01	<0.01	0.08	0.54	0.52	0.73	0.63
La		<0.01	<0.01	<0.01	<0.01	<0.01	<0.01	<0.01	0.02	<0.01	<0.01	<0.01	<0.01
Ce		0.01	<0.01	0.01	<0.01	<0.01	0.29	0.04	0.07	0.01	<0.01	0.01	<0.01
Pr		<0.01	<0.01	<0.01	0.04	0.04	0.16	0.04	0.05	<0.01	<0.01	<0.01	<0.01
Nd		<0.01	<0.01	<0.01	0.69	0.75	1.51	0.71	0.71	<0.01	<0.01	0.04	<0.01
Sm		<0.01	<0.01	<0.01	4.61	5.46	6.59	7.99	8.04	0.14	0.43	0.42	0.13
Eu		<0.01	<0.01	<0.01	<0.01	<0.01	<0.01	0.02	0.04	0.01	0.02	0.03	0.01
Gd		<0.01	<0.01	<0.01	2.08	1.88	1.93	19.12	19.13	0.90	2.06	2.16	0.59
Tb		0.01	0.01	0.01	0.14	0.08	0.07	4.20	4.22	0.47	0.92	1.03	0.30
Dy		0.04	0.05	0.05	0.28	0.11	0.07	12.62	12.77	4.05	6.54	7.61	2.46
Ho		0.01	0.01	0.01	0.02	0.01	<0.01	0.98	1.02	0.63	1.03	1.20	0.38
Er		0.02	0.03	0.02	0.04	0.02	<0.01	2.39	2.45	2.02	2.67	3.18	1.23
Tm		<0.01	<0.01	0.01	0.01	<0.01	<0.01	0.42	0.43	0.44	0.50	0.60	0.27
Yb		0.04	0.05	0.05	0.03	<0.01	<0.01	3.34	3.34	3.98	3.96	4.74	2.60
Lu		0.01	0.01	0.01	<0.01	<0.01	<0.01	0.45	0.46	0.53	0.51	0.60	0.35
Hf		0.70	0.29	0.80	6.21	7.09	8.42	10.06	9.96	1.39	2.14	2.27	0.40
Ta		42.84	49.54	57.38	32.82	42.74	50.44	169.60	143.96	19.82	10.31	11.21	6.84
Pb		0.19	0.20	0.13	<0.01	<0.01	0.19	0.03	0.08	0.16	0.11	0.21	0.19
Th		0.57	0.34	0.69	<0.01	<0.01	0.78	<0.01	0.03	<0.01	0.01	<0.01	<0.01
U		16.85	9.78	17.53	34.10	34.42	19.59	46.40	41.34	18.79	14.73	18.71	7.11
ΣLREE		0.01	<0.01	0.01	5.35	6.25	8.55	8.78	8.89	0.15	0.43	0.48	0.13
ΣHREE		0.13	0.14	0.15	2.58	2.09	2.06	43.56	43.86	13.01	18.21	21.14	8.19

Data of major elements obtained by electron microprobe. Data of trace elements obtained by ICP-MS-LA techniques. The data reported are an average result of point n analyses. The cation numbers are calculated on the basis of 1P per formula unit. Localities: SWA: Swanson pegmatite, T-Q: Tourmaline Queen pegmatite, M-L: Mica Lode pegmatite, and B-B: Black Beauty pegmatite.

TABLE 3 (CONTINUED). CHEMICAL COMPOSITION OF THE MEMBERS OF THE TRIPLITE-ZWIESELITE SERIES FROM DIFFERENT PEGMATITES AND A QUARTZ-RICH DYKE

Sample		CRI-1	CRI-3	CRI-4	GIG-1	GIG-2	GIG-5	FOL-2	FOL 3	FOL 4	HAG-1	HAG-2	HAG-4
n		3	3	3	10	11	10	10	10	10	10	12	11
P_2O_5	wt.%	31.12	31.05	31.47	30.67	31.03	31.28	31.52	31.46	31.34	30.51	30.04	30.86
Al_2O_3		<0.01	0.01	0.03	0.02	0.02	<0.01	<0.01	<0.01	0.01	0.02	0.01	<0.01
MgO		0.83	0.84	0.85	0.01	<0.01	<0.01	2.04	2.25	2.09	0.01	0.02	0.02
FeO		24.21	23.91	24.3	19.35	19.2	19.53	29.4	29.95	28.66	32.95	33.17	34
MnO		34.84	34.66	34.99	40.15	39.83	39.31	32.48	32.2	32.67	28.36	27.75	26.83
CaO		2.51	2.57	2.58	3.19	3.47	3.51	1.48	1.44	1.46	1.08	1.4	1.47
Na_2O		<0.01	0.02	<0.01	0.01	0.05	0.03	<0.01	<0.01	<0.01	0.06	0.01	0.03
K_2O		<0.01	<0.01	<0.01	<0.01	<0.01	<0.01	<0.01	<0.01	<0.01	<0.01	<0.01	<0.01
F		4.27	4.21	4.36	4.52	4.56	4.49	4.12	3.75	3.98	4.06	4.09	4.05
Cl		<0.01	<0.01	<0.01	<0.01	<0.01	<0.01	<0.01	<0.01	<0.01	<0.01	<0.01	<0.01
TOTAL		97.78	97.25	98.59	97.92	98.14	98.15	101.03	101.06	100.19	97.05	96.5	97.26
O = F		1.8	1.77	1.84	1.9	1.92	1.89	1.73	1.58	1.68	1.71	1.72	1.7
total		95.98	95.48	96.75	96.02	96.22	96.26	99.3	99.48	98.52	95.34	94.77	95.56
P	*apfu*	1.000	1.000	1.000	1.000	1.000	1.000	1.000	1.000	1.000	1.000	1.000	1.000
Al		<0.001	<0.001	0.001	0.001	0.001	<0.001	<0.001	<0.001	<0.001	<0.001	<0.001	<0.001
Mg		0.047	0.047	0.048	<0.001	<0.001	<0.001	0.114	0.126	0.117	0.001	0.001	0.001
Fe++		0.768	0.761	0.763	0.623	0.611	0.617	0.921	0.940	0.903	1.067	1.091	1.088
Mn		1.120	1.117	1.113	1.310	1.284	1.257	1.031	1.024	1.043	0.930	0.924	0.870
Ca		0.102	0.105	0.104	0.132	0.141	0.142	0.060	0.058	0.059	0.045	0.059	0.060
Na		<0.001	0.001	<0.001	0.001	0.003	0.002	<0.001	<0.001	<0.001	0.004	0.001	0.002
K		<0.001	<0.001	<0.001	<0.001	<0.001	<0.001	<0.001	<0.001	<0.001	<0.001	<0.001	<0.001
F		0.512	0.506	0.518	0.551	0.549	0.537	0.488	0.445	0.474	0.497	0.509	0.490
Cl		<0.001	<0.001	<0.001	<0.001	<0.001	<0.001	<0.001	<0.001	<0.001	<0.001	<0.001	<0.001

Sample		CRI-1	CRI-3	CRI-4	GIG-1	GIG-2	GIG-5	FOL-2	FOL 3	FOL 4	HAG-1	HAG-2	HAG-4
n		3	3	3	10	11	10	10	10	10	10	12	11
Fe/(Fe+Mn)		0.41	0.41	0.41	0.32	0.32	0.33	0.47	0.48	0.46	0.53	0.54	0.56
Fe/(Fe+Mg)		0.94	0.94	0.94	1	1	1	0.89	0.88	0.89	1	1	1
n		5	5	5	5	5	5	5	5	5	5	5	5
Li	ppm	8.95	13.31	11.47	2.86	1.8	1.88	<0.01	<0.01	<0.01	3.83	9.46	11.7
Sc		0.98	1.07	0.99	0.3	0.37	0.42	14.4	15.08	14.53	2.96	2.81	2.75
V		<0.01	<0.01	<0.01	<0.01	<0.01	<0.01	0.13	0.14	0.15	<0.01	<0.01	<0.01
Cr		0.35	0.47	0.46	0.42	0.62	0.67	0.19	0.26	0.18	0.36	0.36	0.42
Co		3.6	3.85	3.9	1.26	1.34	1.33	0.05	0.04	0.04	0.08	0.09	0.1
Ni		<0.01	<0.01	<0.01	<0.01	<0.01	<0.01	<0.01	<0.01	<0.01	<0.01	<0.01	<0.01
Cu		<0.01	<0.01	<0.01	<0.01	<0.01	<0.01	<0.01	<0.01	<0.01	<0.01	<0.01	<0.01
Zn		900.8	921.4	921	1657.4	1835.2	1921.6	1065	1142	1131	668.6	901	1337.8
Rb		<0.01	<0.01	<0.01	0.15	<0.01	0.03	0.06	0.06	0.01	0.09	0.13	0.11
Sr		0.03	0.03	0.03	0.03	0.03	0.02	0.65	0.58	0.73	<0.01	0.1	0.16
Y		276.92	278.84	275.46	6.89	7.55	7.45	4.6	4.26	4.54	29.89	46.48	48.16
Zr		105.52	109.18	109.16	39.8	44.96	45.92	19.95	20.11	19.94	34.16	233.38	189.62
Nb		217.18	218.34	213.72	79.74	103.18	134.2	93.8	62.3	95.6	135.86	524.6	498.5
Ba		<0.01	<0.01	<0.01	<0.01	<0.01	<0.01	0.03	0.02	0.01	<0.01	1	0.64
La		<0.01	<0.01	<0.01	<0.01	<0.01	0.09	0.02	0.02	0.02	<0.01	<0.01	0.04
Ce		0.11	0.14	0.11	0.97	0.73	0.55	0.09	0.07	0.11	0.01	0.04	0.09
Pr		0.1	0.09	0.08	0.09	0.08	0.08	0.02	0.02	0.02	<0.01	0.02	<0.01
Nd		1.16	1.05	0.99	0.2	0.2	0.2	0.12	0.08	0.11	0.04	0.11	0.14
Sm		2.43	2.42	2.48	0.09	0.1	0.09	0.07	0.05	0.05	0.14	0.39	0.48
Eu		0.05	0.05	0.04	<0.01	<0.01	<0.01	0.04	0.03	0.04	<0.01	<0.01	<0.01
Gd		6.56	7.13	6.24	0.08	0.08	0.09	0.09	0.12	0.12	0.63	1.76	1.96
Tb		2.58	2.73	2.59	0.03	0.04	0.04	0.03	0.03	0.04	0.34	0.77	0.84
Dy		24.82	25.69	24.81	0.34	0.37	0.38	0.36	0.35	0.33	3.1	6.03	6.38
Ho		6.02	5.77	5.57	0.06	0.07	0.07	0.1	0.09	0.1	0.47	0.83	0.85
Er		22.06	23.39	23.06	0.3	0.33	0.34	0.47	0.43	0.43	1.23	2.02	1.87
Tm		4.94	5.36	5.35	0.11	0.13	0.13	0.13	0.11	0.12	0.22	0.31	0.31
Yb		44.06	47.18	46.96	1.49	1.63	1.67	1.33	1.27	1.37	1.51	1.95	1.92
Lu		5.85	6.82	6.72	0.22	0.25	0.25	0.28	0.27	0.26	0.14	0.17	0.18
Hf		3.03	3.14	3.18	1.51	1.71	1.83	0.55	0.54	0.54	1.34	15.17	13.11
Ta		20.15	20.63	20.38	20.19	23.53	32.9	58.1	30.06	57.6	9.39	71.06	68.15
Pb		0.02	0.02	0.02	0.14	0.04	0.04	0.12	0.08	0.21	0.04	0.12	0.06
Th		0.1	0.11	0.09	0.52	0.22	0.32	0.06	0.05	0.10	0.04	0.04	0.02
U		48.08	51.82	47.36	15.72	20.28	24.56	17.7	10.77	18.26	23.66	73.7	67.58
ΣLREE		3.79	3.69	3.65	1.35	1.11	1.01	0.32	0.23	0.31	0.19	0.56	0.75
ΣHREE		116.93	124.12	121.35	2.63	2.89	2.97	2.83	2.69	2.81	7.64	13.84	14.3

Data of major elements obtained by electron microprobe. Data of trace elements obtained by ICP-MS-LA techniques. The data reported are an average result on n point analyses. The cation numbers are calculated on the basis of 1P per formula unit.
Localities: CRI: E1 Criollo pegmatite, GIG: Gigante pegmatite, FOL: Folgosinho quartz-dyke, HAG: Hagendorf Süd pegmatite.

TABLE 4. CHEMICAL COMPOSITION OF THE MEMBERS OF THE GRAFTONITE-BEUSITE SERIES FROM DIFFERENT PEGMATITES

Sample		CEM-1	CEM-3	CEM-6	CEM-9	PAL-3	PAL-6	PAL-7	PAL-8	PAL-9	KEY-8	KEY-6	KEY-3	KEY-4	KEY-1	S-M-2	S-M-4
n		3	3	3	3	5	6	10	10	11	12	14	13	10	10	3	3
P_2O_5	wt.%	40.96	40.55	40.10	40.58	41.41	41.07	40.31	40.60	40.44	39.06	39.21	37.95	38.83	39.25	39.09	39.22
Al_2O_3		0.01	0.02	0.04	0.02	<0.01	0.01	0.01	0.01	<0.01	<0.01	<0.01	0.01	0.01	0.01	0.03	0.02
TiO_2		<0.01	<0.01	<0.01	<0.01	<0.01	<0.01	<0.01	<0.01	<0.01	<0.01	<0.01	<0.01	<0.01	<0.01	<0.01	<0.01
MgO		0.62	0.73	0.85	0.63	1.07	1.04	1.07	1.02	0.66	0.20	0.22	0.18	0.18	0.19	0.32	0.32
FeO		18.52	18.25	18.75	18.34	28.11	28.10	27.90	27.55	26.49	26.00	25.63	25.76	25.54	25.61	21.65	21.88
MnO		33.92	32.71	33.20	33.45	15.16	15.32	15.15	15.28	18.97	26.45	26.52	26.41	26.37	26.28	28.83	29.9
CaO		6.19	7.35	6.01	5.89	13.14	13.14	13.28	13.49	10.97	5.87	6.24	6.14	6.47	6.45	6.95	6.32
Na_2O		<0.01	0.02	0.06	0.06	0.01	0.01	0.03	0.02	0.03	0.04	0.04	0.03	0.03	0.03	0.03	0.03

Sample		CEM-1	CEM-3	CEM-6	CEM-9	PAL-3	PAL-6	PAL-7	PAL-8	PAL-9	KEY-8	KEY-6	KEY-3	KEY-4	KEY-1	S-M-2	S-M-4
n		3	3	3	3	5	6	10	10	11	12	14	13	10	10	3	3
K_2O		0.01	0.01	<0.01	<0.01	0.01	<0.01	<0.01	<0.01	<0.01	0.01	0.01	0.01	0.01	0.01	0.01	0.01
TOTAL		100.22	99.64	99.01	98.97	98.89	98.70	97.75	97.98	97.55	97.63	97.86	96.48	97.43	97.81	96.91	97.71
P	*apfu*	2.000	2.000	2.000	2.000	2.000	2.000	2.000	2.000	2.000	2.000	2.000	2.000	2.000	2.000	2.000	2.000
Al		<0.001	0.001	0.003	0.001	<0.001	<0.001	0.001	<0.001	<0.001	<0.001	<0.001	0.001	0.001	0.001	0.002	0.002
Ti		<0.001	<0.001	<0.001	<0.001	<0.001	<0.001	<0.001	<0.001	<0.001	<0.001	<0.001	<0.001	<0.001	<0.001	<0.001	<0.001
Mg		0.054	0.063	0.075	0.055	0.091	0.089	0.093	0.089	0.057	0.018	0.019	0.017	0.017	0.017	0.029	0.029
Fe^{++}		0.893	0.889	0.924	0.893	1.341	1.352	1.367	1.341	1.294	1.315	1.291	1.341	1.299	1.289	1.094	1.102
Mn^{++}		1.657	1.614	1.656	1.649	0.733	0.747	0.752	0.753	0.939	1.355	1.353	1.392	1.358	1.340	1.476	1.525
Ca		0.382	0.459	0.380	0.368	0.803	0.810	0.834	0.841	0.687	0.380	0.403	0.409	0.422	0.416	0.450	0.408
Na		<0.001	0.002	0.007	0.007	0.001	0.002	0.003	0.003	0.003	0.004	0.004	0.003	0.003	0.003	0.004	0.004
K		<0.001	0.001	<0.001	<0.001	<0.001	<0.001	<0.001	<0.001	<0.001	<0.001	0.001	<0.001	0.001	<0.001	0.001	0.001
Fe/(Fe+Mn)		0.35	0.36	0.36	0.35	0.65	0.64	0.65	0.64	0.58	0.49	0.49	0.49	0.49	0.49	0.43	0.42
Fe/(Fe+Mg)		0.94	0.93	0.92	0.94	0.94	0.94	0.94	0.94	0.96	0.99	0.99	0.99	0.99	0.99	0.97	0.97
n		5	5	5	5	5	5	5	5	5	5	5	5	5	5	5	5
Li	ppm	18.57	6.62	4.76	7.62	3.70	Bdl	Bdl	Bdl	6.70	10.80	9.84	2.67	2.66	1.25	Bdl	9.62
Sc		0.38	0.46	0.29	0.35	3.96	5.03	4.93	4.44	4.69	1.96	2.11	2.07	1.79	1.90	0.69	0.61
V		Bdl	103.09	Bdl	1.46	Bdl	Bdl	Bdl	Bdl	Bdl	Bdl	Bdl	Bdl	Bdl	Bdl	Bdl	Bdl
Cr		0.58	0.59	0.58	0.60	Bdl	0.48	0.32	Bdl	0.52	0.91	1.04	1.02	0.86	0.82	0.49	0.52
Co		0.37	0.36	0.38	0.43	0.08	0.16	0.09	0.08	0.26	0.30	0.27	0.28	0.29	0.24	2.07	2.10
Ni		Bdl	Bdl	Bdl	Bdl	Bdl	Bdl	Bdl	Bdl	Bdl	Bdl	Bdl	Bdl	Bdl	Bdl	Bdl	Bdl
Cu		Bdl	Bdl	Bdl	Bdl	1.20	Bdl	0.73	2.01	Bdl	Bdl	Bdl	Bdl	Bdl	Bdl	Bdl	Bdl
Zn		1596	1563	1742	1875	2434	2078	2123	2155	2930	1782	1830	1887	1937	1731	4238	4040
Rb		0.37	0.32	0.22	0.22	0.13	0.10	Bdl	0.25	0.31	Bdl	Bdl	0.08	0.02	1.21	0.48	0.24
Sr		33.48	171.90	10.70	27.01	5.05	5.71	2.23	4.45	39.50	3.01	2.92	3.11	4.55	3.75	16.53	17.39
Y		0.06	0.05	0.09	0.06	509.60	156.24	167.36	213.92	12.67	245.32	257.44	264.02	231.54	193.02	28.94	28.03
Zr		Bdl	Bdl	Bdl	Bdl	Bdl	0.25	0.28	Bdl	0.36	Bdl	0.09	0.06	Bdl	Bdl	Bdl	Bdl
Nb		Bdl	Bdl	Bdl	Bdl	0.09	0.07	0.05	0.06	0.11	0.03	0.05	0.05	0.03	0.03	Bdl	Bdl
Ba		0.58	58.53	0.97	4.90	0.55	0.47	0.19	1.63	Bdl	Bdl	Bdl	Bdl	1.83	Bdl	Bdl	Bdl
La		0.09	0.10	0.41	0.06	7.26	21.96	18.11	17.33	46.80	17.33	19.31	21.47	12.39	13.46	11.21	14.12
Ce		0.50	0.51	1.41	0.32	65.18	91.56	78.80	73.74	109.83	83.88	91.22	96.30	70.94	76.54	44.65	69.43
Pr		0.08	0.07	0.14	0.05	14.77	12.33	12.19	11.58	9.50	16.68	18.38	18.98	15.94	15.19	6.67	8.84
Nd		0.24	0.18	0.29	0.16	75.68	41.08	42.72	41.08	16.54	86.40	94.08	95.64	84.84	79.86	21.38	22.66
Sm		0.12	0.09	0.12	0.09	45.52	15.90	18.61	2<0.01	1.50	107.26	122.42	121.36	109.68	96.38	6.20	6.24
Eu		<0.01	<0.01	<0.01	<0.01	3.40	2.25	2.30	2.29	0.87	0.05	0.05	0.05	0.05	0.04	0.01	0.02
Gd		0.09	<0.01	0.06	0.07	58.74	14.93	16.53	20.92	0.73	147.48	162.02	158.46	142.38	133.36	2.49	2.56
Tb		<0.01	<0.01	0.01	<0.01	15.75	4.12	4.56	5.90	0.15	30.25	33.52	33.72	<0.01	25.74	0.62	0.62
Dy		<0.01	<0.01	<0.01	<0.01	101.06	26.52	28.84	37.94	0.93	95.98	103.94	100.60	89.90	80.72	3.07	3.08
Ho		<0.01	<0.01	<0.01	<0.01	14.15	3.50	3.68	5.11	0.13	3.60	3.91	3.74	3.28	2.89	0.28	0.29
Er		<0.01	<0.01	<0.01	<0.01	36.12	9.62	9.93	13.46	0.53	2.40	2.53	2.43	2.16	1.89	0.80	0.81
Tm		<0.01	<0.01	<0.01	<0.01	5.76	1.80	1.93	2.46	0.20	0.19	0.19	0.18	0.17	0.15	0.24	0.24
Yb		<0.01	<0.01	<0.01	<0.01	37.86	13.42	15.61	18.73	3.01	1.08	1.06	1.00	0.97	0.88	2.83	2.76
Lu		<0.01	<0.01	<0.01	<0.01	4.12	1.58	1.77	2.14	0.54	0.14	0.14	0.13	0.13	0.11	0.37	0.36
Hf		Bdl	Bdl	Bdl	Bdl	0.03	Bdl	Bdl	Bdl	Bdl	0.02	0.03	0.03	Bdl	0.02	Bdl	Bdl
Ta		Bdl	Bdl	Bdl	Bdl	0.01	0.01	0.01	Bdl	Bdl	0.02	0.09	0.03	0.01	0.01	Bdl	Bdl
Pb		2.38	5.32	0.45	0.36	8.20	6.00	5.73	6.04	3.87	4.75	4.67	4.83	4.84	5.28	0.49	0.89
Th		0.01	0.01	Bdl	0.02	0.03	0.02	Bdl	Bdl	0.10	0.10	0.24	0.49	0.02	0.02	Bdl	Bdl
U		0.05	5.63	0.11	0.13	0.66	8.25	0.95	0.32	6.70	5.60	4.55	10.16	3.18	3.43	0.14	0.46
ΣLREE		1.03	0.95	2.36	0.68	208.42	182.83	170.44	163.74	184.16	311.56	345.40	353.75	293.79	281.44	90.12	121.28
ΣHREE		0.09	<0.01	0.07	0.07	276.95	77.76	85.16	108.96	7.09	281.16	307.36	300.32	269.04	245.79	10.72	10.74

Data of major elements obtained by electron microprobe. Data of trace elements obtained by ICP-MS-LA techniques. The data reported are an average result on n point analyses. The cation numbers are calculated on the basis of 2P per formula unit. Localities: CEM: Cema pegmatite, PAL: Palermo 1 pegmatite, KEY: Keystone pegmatite, and S-M: Storm Mountain pegmatite. Bdl: below detection limits.

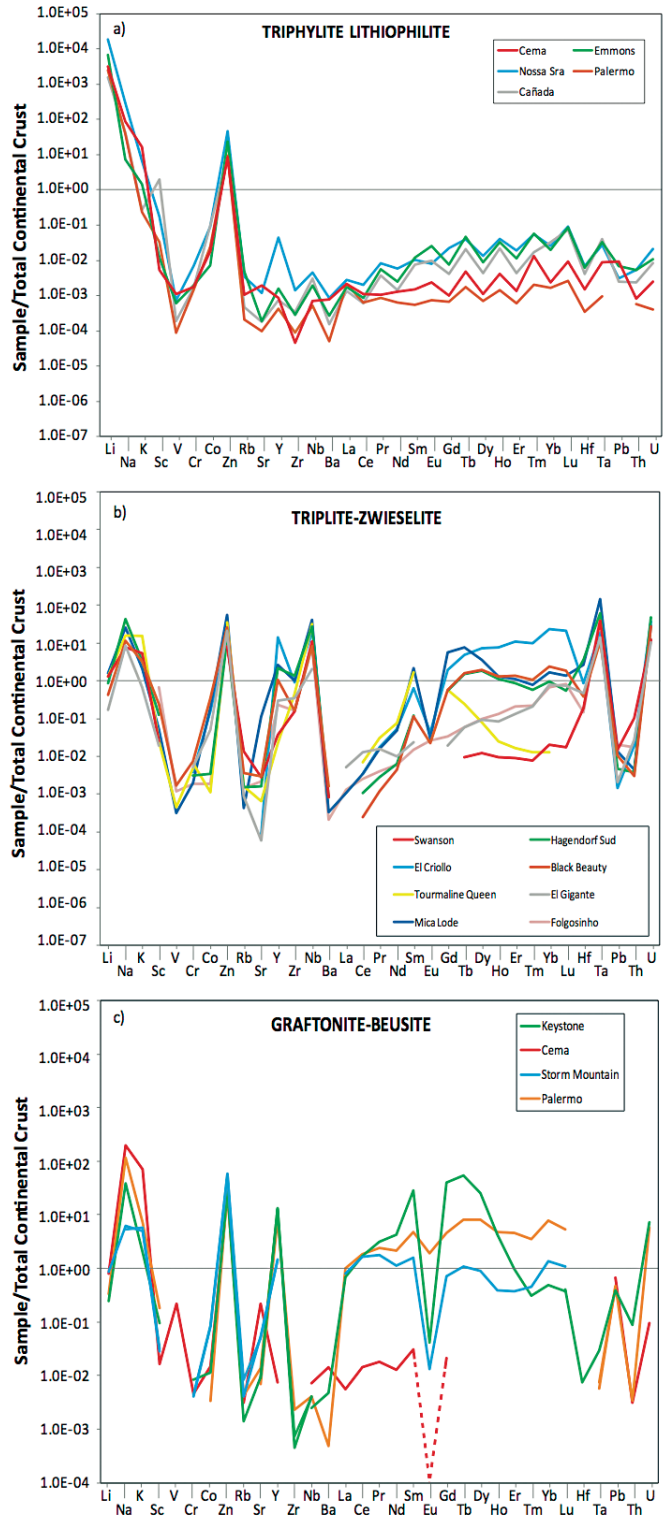

FIG. 2. Analyzed element concentrations for (a) triphylite-litiophilite, (b) triplite-zwieselite, and (c) graftonite-beusite, normalized to Total Continental Crust (Rudnick & Fountain 1995). Some elements, mainly in samples of graftonite-beusite from the Cema pegmatite, are below detection limit and are represented by a dotted line.

lithiophilite series (Table 3, Figs. 2, 3); with high Zn (437–4093 ppm) and Nb (62–37 ppm) contents; and variable amounts of heavy rare earth elements (ΣHREE = 0–124 ppm), Ta (4–176 ppm), Y (0–280 ppm), Zr (6–233 ppm), U (7–74 ppm), and Hf (0.5–15 ppm). Most samples from the different localities show a good positive correlation between Nb and the high field strength elements (HFSE) Ta, U, Zr, and Hf, and the light rare earth elements (LREE), Li, and Zn, with *R* values > 0.82 for all them (Table 3, Figs. 3a–g). Zirconium and Hf also show a good positive correlation (*R* = 0.90) (Fig. 3h). The lowest Zr/Hf ratios correspond to the samples from the Mica Lode and Tourmaline Queen pegmatites, which are also the richest in Nb+Ta, LREE, Li, and Zn, whereas samples from Hagendorf Süd are the richest in both Zr and Hf (Table 3, Fig. 3a, e, f, g). As for the triphylite-lithiophilite series, no correlation was found between the Fe/(Fe+Mn) ratio and any trace element. In the multi-element diagram plot (Fig. 2b) the lack of a negative Eu anomaly for the samples associated with the quartz-rich dike of Folgosinho is remarkable.

Samples of the graftonite-beusite series are clearly richer in REE than the two other phosphate mineral series, with ΣHREE up to 300 ppm and of ΣLREE up to 345 ppm (Table 4, Figs. 2c, 4). Other trace elements, such as Zn (1508–4238 ppm), Sr (3–91 ppm), and Y (0–509 ppm) also occur in significant amounts in the graftonite-beusite samples. Certain correlations among the ΣLREE values and other elements such as ΣHREE, Fe, Y, and Zn were found for some of the pegmatites (Fig. 4). Samples from Keystone are the richest in REE and Y, with low Zn contents, whereas those from Cema and Storm Mountain are the poorest in REE, Y, and Fe. The highest Zn contents in graftonite-beusite were found in the samples from Storm Mountain (Table 4, Fig. 4). In the multi-elemental diagram, all the analyzed samples of the graftonite-beusite series show a similar shape, with a strong Eu negative anomaly (Fig. 2c).

Discussion

Important variations in the trace element contents have been observed among the three series of primary phosphate minerals analyzed in this study. In turn, multi-element diagrams for samples belonging to the same series are remarkably similar (Fig. 2). This suggests that chemical variations are controlled to a great extent by the crystal structure of the phosphate minerals, rather than by the bulk composition of the pegmatitic melt. This appears evident in cases where members of different phosphate mineral series occur together, as in the Palermo no.1 pegmatite. There, triphylite and graftonite appear in an intimate intergrowth, but both present quite different concentrations of trace elements (Tables 2, 3, 4; Fig. 2a, c). The higher REE content of the graftonite-beusite, if compared with the other two series, is most probably due to the replacement of Ca at the seven-fold coordination M1 positions, as described by Calvo (1968). There are also important differences in trace element content between the triphylite-lithiophilite and triplite-zwesielite series. Whereas triplite-zwieselite members are relatively enriched in some trace elements, mainly HFSE, the triphylite-lithiophilite phosphate minerals are extremely poor in all traces, with the exception of Zn. The Fe and Mn atoms occupy octahedral positions in both series (Waldrop 1969, Losey *et al*. 2004), however, the replacement of Fe-Mn by HFSE is not operative in the structures of the triphylite-lithiophilite minerals. This could be due to crystal-chemical constraints, difficult to determine at the present level of knowledge. Another explanation could be the presence of inclusions in the triplite-zwieselite minerals. Certainly, in Figure 1a the presence of multiple inclusions is evident. However, this is not the case for all eight samples of triplite-zwieselite analyzed in this study. Moreover, analyses were always obtained from areas of the crystals where no inclusions were observed under the microscope (50×).

On the other hand, a broad range in the content of some trace elements was also observed in every series, in particular in the triplite-zwieselite and graftonite-beusite series (Figs. 2, 3, 4). In fact, the different shapes of the multi-element diagrams from the triplite-zwieselite samples associated with pegmatites are remarkable, in that all of them show a strong negative Eu anomaly, whereas those associated with the quartz-rich dike of Folgosinho, present, in contrast, no Eu anomaly (Fig. 2b). This difference is interpreted as the result of the Eu fractionation in pegmatites due to the previous crystallization of plagioclase. The lack of this phase in the quartz dike would prevent such Eu fractionation in the samples from Folgosinho. Other differences in the trace-element contents for a given series are more difficult to understand. There is no correlation, for example, between the Fe/(Fe+Mn) ratio and the different trace element contents (Tables 2, 3, 4). Also, the plots of some of the most abundant trace elements in the different series by pairs of elements yield relatively poor correlations up to *ca*. 0.82 (Figs. 3, 4), which indicates that the concentrations are not simply related to the pegmatite type, the paragenesis, or geological setting. In the case of the triplite-zwieselite series, the highest contents in Nb, Ta, LREE, and Li are shown by triplites from Mica Lode, whereas the lowest values of these elements correspond to Black Beauty and Gigante, all three belonging to the beryl-columbite-phosphate subtype. Similarly, triplite from Tourmaline Queen is one of the richest in those trace elements, whereas Swanson is one of the poorest, the two bodies being Li-rich complex pegmatites, and, therefore, highly fractionated. Consequently, the interpretation of the trace element distribution in these primary phosphate minerals is not simple. Further investigation of mineral association,

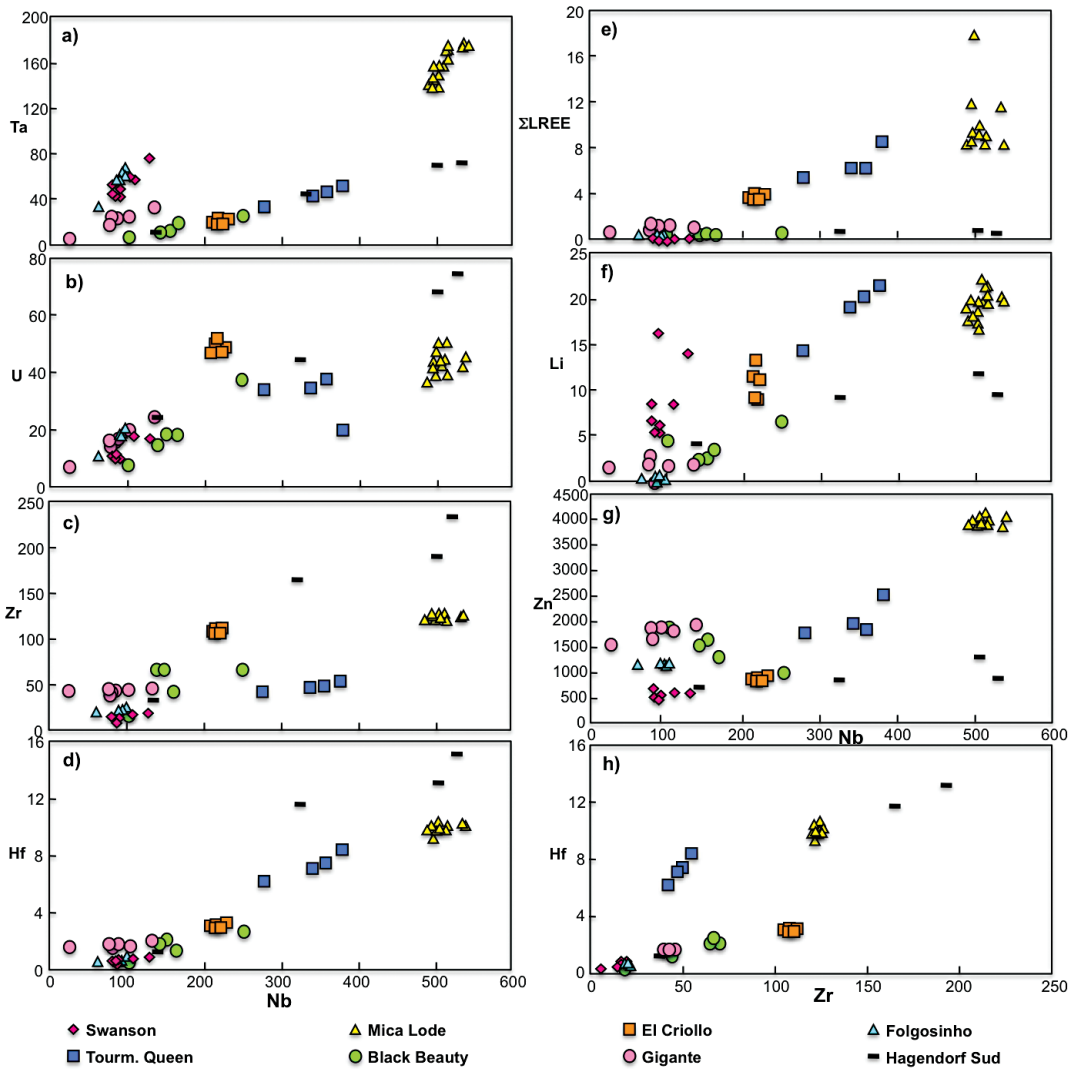

FIG. 3. Plot of Nb *versus* (a) Ta, (b) U, (c) Zr, (d) Hf, (e) ΣLREE, (f) Li, and (g) Zn; and (h) plot of Zr *versus* Hf (*apfu*) for members of the triplite-zwieselite series associated with different pegmatites.

textural relationships, geology, and history of crystallization of the pegmatitic bodies would be necessary in order to determine (1) the factors that control the variability in trace element content for the different primary phosphate mineral series; (2) the distribution coefficients between phosphate minerals and coexisting silicate minerals such as biotite, tourmaline, and garnet; and (3) the influence of the source of the pegmatites and bulk composition on the geochemistry of the primary Fe-Mn phosphate minerals.

CONCLUSIONS

The following conclusions can be made concerning the trace element contents of primary Fe-Mn phosphate minerals belonging to the triphylite-lithiophilite, graftonite-beusite, and triplite-zwieselite series, associated with different pegmatites and a quartz-rich dike:

(1) The concentration of trace elements shows important differences for the three series of Fe-Mn phosphate minerals. Members of the triphylite-

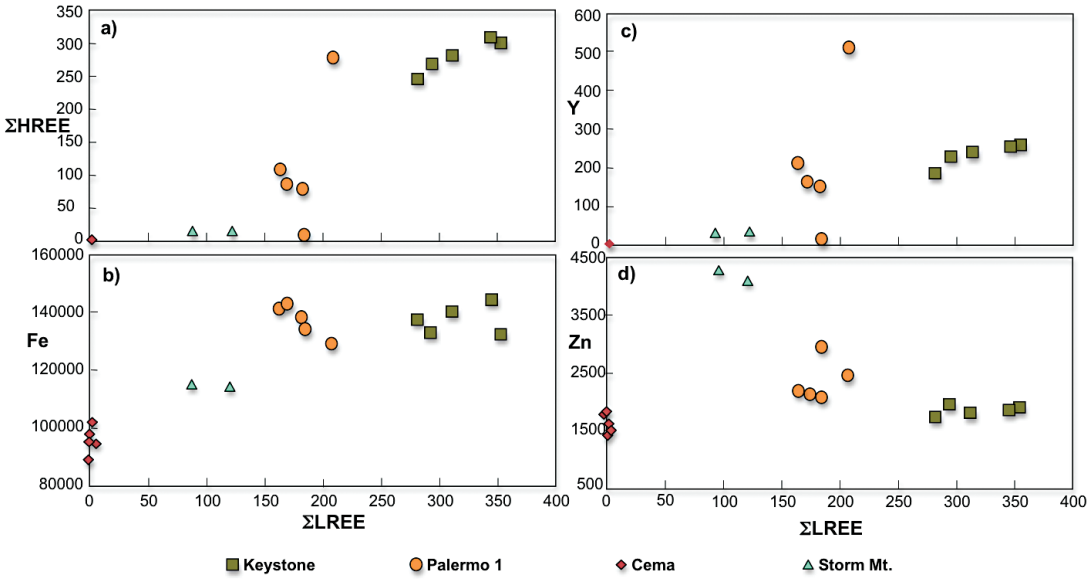

FIG. 4. Plot of ΣLREE *versus* (a) ΣHREE, (b) Y, (c) Fe, and (d) Zn, (*apfu*) for members of the graftonite-beusite series associated with different pegmatites.

lithiophilite series are the poorest in trace elements, with Zn as the only element that may occur in important amounts. Graftonite-beusite members are the richest in REE, whereas members of the triplite-zwieselite series are the richest in certain HFSE, such as Nb and Ta.

(2) The differences in trace element contents for the different phosphate mineral series seem to be controlled, in a great extent, by crystal-chemical factors.

(3) There are also important differences in trace element contents in phosphate minerals depending on the hosting pegmatite or quartz-rich dike. In some cases these chemical differences seem directly related to the paragenesis or geological setting, as for the triplite-zwieselite samples associated with pegmatites or with a quartz-rich dike. However, in general, the concentrations of trace elements are not simply related to the pegmatite type, its paragenesis, or its geological setting.

(4) No correlation has been found between the Fe/(Fe+Mn) ratio and the different trace element contents of the primary phosphate mineral series analyzed in this study.

(5) Laser-ablation inductively coupled-plasma mass-spectrometry (LA-ICP-MS) seems to be a good technique for analyzing trace elements in phosphates. However, it is necessary to pay attention to the possible occurrence of inclusions inside some of the studied phases.

ACKNOWLEDGEMENTS

The authors thank two anonymous referees for thorough reviews and comments that have greatly helped to improve the manuscript. The authors want to express their gratitude to Dr. François Fontan, Prof. Paul Keller, and Prof. André-Mathieu Fransolet, whose numerous works on phosphates associated with pegmatites have greatly contributed to the study and understanding of these mineral phases. Dr. Roda-Robles is especially indebted to Dr. François Fontan, who was her mentor and friend, and passed onto her his enthusiasm for the study of phosphates. This research has been financially supported by the Spanish Ministerio de Economia y Competitividad (Projects CGL2008-01130/BTE and CGL2012-31356 with ERDF funds), and the Universidad del País Vasco UPV/EHU (Project GIU09/61).

REFERENCES

CALVO, C. (1968) The crystal structure of graftonite. *American Mineralogist* **53**, 742–750.

ČERNÝ, P. & ERCIT, T. S. (2005) The classification of granitic pegmatites revisited. *Canadian Mineralogist* **43**, 2005–2026.

FRANSOLET, A.M., KELLER, P., & FONTAN, F. (1986) The phosphate mineral associations of the Tsaobismund pegmatite, Namibia. *Contributions to Mineralogy and Petrology* **92**, 502–517.

Garate-Olabe, I., Roda-Robles, E., Gil-Crespo, P.P., Pesquera-Pérez, A., Vieira, R., & Lima, A. (2012) Estudio textural y mineralógico del dique de cuarzo con fosfatos de Folgosinho (Guarda, Portugal). *Macla* **16**, 220–221.

Ginsburg, A.I. (1960) Specific geochemical features of the pegmatitic process. *21st International Geological Congress Session Norden Report* **Part 17**, 111–121.

Keller, P., Fontan, F., & Fransolet, A.M. (1994) Intercrystalline cation partitioning between minerals of the triplite-zwieselite-magniotriplite and the triphylite-lithiophilite series in granitic pegmatites. *Contributions to Mineralogy and Petrology* **118**, 239–248.

London, D. (2008) Pegmatites. *Mineralogical Association of Canada, Special Publication* **10**.

London, D. & Burt, D.M. (1982) Alteration of spodumene, montebrasite and lithiophilite in pegmatites of the White Picacho District, Arizona. *American Mineralogist* **67**, 494–509.

Losey, A., Rakovan, J., & Hughes, J.M. (2004) Structural variation in the lithiophilite-triphylite series and other olivine-group structures. *Canadian Mineralogist* **42**, 1105–1115.

Mason, B. (1941) Minerals of the Varuträsk pegmatite. XXIII. Some iron-manganese phosphate minerals and their alteration products, with special reference to material from Varutrask. *Geologiska Foreningen i Stockholm Forhandlingar* **63**, 117–175.

Paton, C., Hellstrom, J., Paul, B., Woodhead, J., & Hergt, J. (2011) Iolite: Freeware for the visualisation and processing of mass spectrometric data. *Journal of Analytical Atomic Spectrometry* **26**, 2508–2518.

Paul, B., Paton, C., Norris, A., Woodhead, J., Hellstrom, J., Hergt, J., & Greig, A. (2012) CellSpace: A module for creating spatially registered laser ablation images within the Iolite freeware environment. *Journal of Analytical Atomic Spectrometry* **27**, 700–706.

Quensel, P. (1937) Minerals of the Varuträsk pegmatite. I: The lithium-manganese phosphates. *Geologiska Foreningen i Stockholm Forhandlingar* **59**, 77–96.

Roda, E., Pesquera, A., Gil-Crespo, P.P., Torres-Ruiz, J., & Fontan, F. (2005) Origin and internal evolution of the Li–F–Be–B–P-bearing Pinilla de Fermoselle pegmatite (Central Iberian Zone, Zamora, Spain). *American Mineralogist* **90**, 1887–1899.

Roda-Robles, E., Vieira, R., Pesquera, A., & Lima, A. (2010) Chemical variations and significance of phosphates from the Fregeneda-Almendra pegmatite field, Central Iberian Zone (Spain and Portugal). *Mineralogy and Petrology* **100**, 23–34.

Roda-Robles, E., Galliski, M.A., Roquet, M.B., Hatert, F., & de Parseval, P. (2012) Phosphate nodules containing two distinct assemblages in the Cema granitic pegmatite, San Luis province, Argentina: paragenesis, composition and significance in the pegmatite evolution. *Canadian Mineralogist* **50**, 913–931.

Rudnick, R.L. & Fountain, D.M. (1995) Nature and composition of the continental crust: A lower crustal perspective. *Reviews of Geophysics* **33(3)**, 267–309.

Waldrop, L. (1969) The crystal structure of triplite, $(Mn,Fe)_2FPO_4$. *Zeitschrift für Kristallographie* **130**, 1–14.

Received February 11, 2014. Revised manuscript accepted March 24, 2014.